International Journal of Engineering Science 47 (2009) 610–617

Contents lists available at ScienceDirect

International Journal of Engineering Science

journal homepage: www.elsevier.com/locate/ijengsci

On the negative effective mass density in acoustic metamaterials

H.H. Huang [a], C.T. Sun [a,*], G.L. Huang [b]

[a] School of Aeronautics and Astronautics, Purdue University, W. Lafayette, IN 47907, USA
[b] Department of Systems Engineering, University of Arkansas at Little Rock, Little Rock, AR, 72204, USA

ARTICLE INFO

Article history:
Received 19 October 2008
Received in revised form 5 December 2008
Accepted 19 December 2008
Available online 31 January 2009

Keywords:
Lattice
Acoustic metamaterials
Left-handed metamaterials
Negative effective mass density
Local resonance
Multi-displacement continuum theory

ABSTRACT

In this paper, we demonstrate the consequence of using different equivalent models to represent a lattice system consisting of mass-in-mass units and why negative mass is needed in the equivalent model. Dispersive wave propagation in the lattice system is studied and compared to various equivalent models. It is found that, if the classical elastic continuum is used to represent the original mass-in-mass lattice system, the effective mass density becomes frequency dependent and may become negative for frequencies near the resonance frequency of the internal mass. In contrast, if a multi-displacement microstructure continuum model is used to represent the mass-in-mass lattice system, the dispersive behavior of wave propagation and the band gap structure can be adequately described. However, while the acoustic mode is accurately described by the microstructure continuum model, the description of the optical mode is accurate only for a limited frequency range.

1. Introduction

Recently, the subject of left-handed metamaterials has attracted much attention of researchers. The idea of metamaterials with negative properties traces back to 1968 when Veselago [1] postulated a theory for possible materials having negative electric permittivity (ε) and magnetic permeability (μ), and hence resulting in a negative refractive index. However, this concept did not stimulate much interest among researchers at that time. In 2000, Pendry [2] first proposed the theoretical possibility of making left-handed electromagnetic metamaterials. Since then, many researchers have been engaged in exploring negative index metamaterials with various potentially novel applications [3].

Motivated by the mathematical analogy between acoustic and electromagnetic waves, some researchers have attempted to find the counterpart left-handed acoustic metamaterials. Basically, it is to find metamaterials that possess negative mass density and negative modulus [4–8]. However, in contrast to the natural negative electric permittivity, no natural material has been found to possess negative mass density or negative modulus. Ever since the investigation on locally resonant acoustic materials [9], some new developments have further been theoretically attempted and shown that metamaterials with certain manmade microstructures may exhibit negative mass/mass density if treated as a classical elastic solid [10,11]. Recently, Lazarov and Jensen [12] have studied the wave propagation on a locally resonant lattice model which was originally introduced by Vincent [13] for use as a possible mechanical filter. Yao et al. [14] have conducted experiments using a 1D spring-mass system to demonstrate the effect of the negative effective mass on the dynamic transmission in the spring-mass system. In short, the frequency region in connection with negative mass creates a band gap effect.

There is no actual negative mass/mass density in real materials indeed. The negative effective mass/mass density is the result of inaccurate modeling of acoustic metamaterials. In the present study, we consider a one-dimensional lattice consisting of lattice masses each of which contains an internal mass. This simple lattice system is employed to illustrate how the

* Corresponding author. Tel.: +1 765 494 5130; fax: +1 765 494 0307.
E-mail address: sun@purdue.edu (C.T. Sun).

0020-7225/$ - see front matter © 2009 Elsevier Ltd. All rights reserved.
doi:10.1016/j.ijengsci.2008.12.007

negative effective mass could occur and what effects it has on wave propagation in the lattice system. We also show that the conventional continuum theory is not adequate in describing the micromotion in this system and a so-called Cosserat type of microstructure continuum model [15–17] is more suitable to represent the lattice system. From the framework of the microstructure continuum representation of acoustic metamaterials, no negative mass density is present while the band gap structure is accurately described.

2. Negative effective mass in lattice

Chan et al. [8] as well as Milton and Willis [11] had employed a one-dimensional model to introduce the negative effective mass effect. Both of their model was based on those of Sheng et al. [18] and Liu et al. [10]. A similar mass-in-mass unit is shown in Fig. 1. If it is to be represented by a single mass, then the effective mass must be defined in order that the effective mass m_{eff} would produce the same motion of m_1. In other words, the identity of the internal mass $m_2$would be ignored and its effect would be absorbed by the introduction of an effective mass m_{eff} as depicted in Fig. 1. Solving the equations of motion for these two dynamically equivalent units subjected to a sinusoidal force of amplitude $\hat{F}$, we readily obtain the displacement amplitude $\hat{u}_1$ so that

$$\hat{u}_1 = -\frac{\hat{F}}{m_{eff}\omega^2} \tag{1}$$

where

$$m_{eff} = m_1 + \frac{m_2\omega_0^2}{\omega_0^2 - \omega^2} \tag{2}$$

represents the effective mass and $\omega_0 = \sqrt{k_2/m_2}$ is the local resonance frequency of m_2. The expression above indicates that the effective mass is a function of $(\omega_0^2 - \omega^2)^{-1}$ and is highly dependent of the local resonance frequency ω_0. It is evident that, when the forcing frequency ω approaches ω_0 from above, the effective mass becomes negative. In fact, the magnitude of the effective mass would become unbounded at the frequency ω_0. It is of interest to note that, if the mass becomes negative, the acceleration would be in the opposite direction to the applied force according to the Newton's second law of motion, and the response amplitude would be reduced. This effect is greatly magnified as the input frequency approaches the local resonance frequency. Moreover, it is clear that the negativity of the effective mass is the result of our attempt to use a single mass to represent a two-mass system.

For wave transmission, we consider an infinitely long one-dimensional lattice system consisting of mass-in-mass lattice points as shown in Fig. 2, which resembles those of Chan et al. [8] as well as Milton and Willis [11]. Apparently, this lattice system is constructed by connecting the unit cells of Fig. 1 with linear springs. The unit-cells are placed periodically at a spacing of L. Harmonic wave propagation in the mass-in-mass lattice system is considered. The equations of motion for the j-th unit cell are

$$m_1^{(j)}\frac{d^2u_1^{(j)}}{dt^2} + k_1(2u_1^{(j)} - u_1^{(j-1)} - u_1^{(j+1)}) + k_2(u_1^{(j)} - u_2^{(j)}) = 0 \tag{3}$$

$$m_2^{(j)}\frac{d^2u_2^{(j)}}{dt^2} + k_2(u_2^{(j)} - u_1^{(j)}) = 0 \tag{4}$$

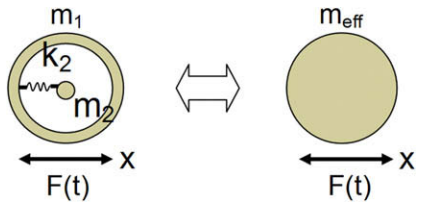

Fig. 1. Single spring-mass system and its effective single mass model.

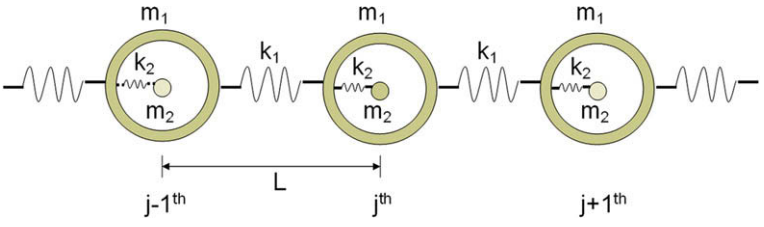

Fig. 2. Infinite mass-in-mass lattice structure.

where $u_\gamma^{(j)}$ represents the displacement of mass "γ" in the j-th cell. The harmonic wave solution for the $(j+n)$th unit cell is expressed in the form

$$u_\gamma^{(j+n)} = B_\gamma e^{i(qx+nqL-\omega t)} \tag{5}$$

where B_γ is complex wave amplitude, q is wave number, ω is angular frequency, and $\gamma = 1$ and 2. The substitution of Eq. (5) in Eqs. (3) and (4) yields two homogeneous equations for B_1 and B_2 from which the dispersion equation is obtained as

$$m_1 m_2 \omega^4 - [(m_1+m_2)k_2 + 2m_2 k_1(1-\cos(qL))]\omega^2 + 2k_1 k_2(1-\cos(qL)) = 0 \tag{6}$$

Two branches of the band structure can be obtained according to Eq. (6). Fig. 3 shows the dispersion curves for a specific set of material constants:

$$m_2/m_1 = 9, \quad k_2/k_1 = 0.1, \text{ and } \omega_0 = \sqrt{k_2/m_2} = 149.07 \text{ rad/s } (= 23.73 \text{ Hz}) \tag{7}$$

Comparing this result with that of the typical diatomic lattice model (for example, Kelvin's model cited by Brillouin [19]), some differences are observed. First, the dispersion curve of the optical mode according to the present model concaves up, while according to the Kelvin's model it concaves down. Second, the range of the passing band in the optical mode predicted by the current model is significantly wider than that for the Kelvin's model.

In Fig. 4, we plot the dimensionless wave number with respect to wave frequency. The result gives the wave number a complex number and is plotted in the form of $qL = \alpha + i\beta$, where α and β are the dotted and solid lines, respectively. Note that the displacements in Eq. (5) are function of e^{iqx}. Substituting $qL = \alpha + i\beta$ into (5) yields

$$u_\gamma \propto e^{i(\alpha+i\beta)(x/L)} = e^{-\beta(x/L)} e^{i\alpha(x/L)} \tag{8}$$

The amplitude of the displacement is proportional to $e^{-\beta(x/L)}$, and, thus, the displacement decays spatially as an exponential function if the attenuation factor β is positive. Of particular interest is that when wave frequency approaches the local resonance frequency ω_0, the attenuation factor β theoretically becomes unbounded. In other words, the spatial wave attenuation effect is maximized by the local resonance. The same conclusion has also been reached by Lazarov and Jensen [12].

Next, consider an effective monatomic lattice system in which only effective masses m_{eff} are connected by springs with spring constant k_1. For this homogeneous lattice system the dispersion equation is readily obtained as

$$\omega^2 = \frac{2k_1(1-\cos(qL))}{m_{eff}} \tag{9}$$

If this effective monatomic lattice system is equivalent to the original mass-in-mass lattice system, then the dispersion curves of the two systems must be identical. In other words, in Eq. (9) the effective mass m_{eff} must be selected so that the relation between ω and qL is same as that for the original mass-in-mass system. This requirement is used to determine the effective mass. We obtain

$$m_{eff} = m_{st} + \frac{m_2(\omega/\omega_0)^2}{1-(\omega/\omega_0)^2} \tag{10}$$

where $m_{st} = m_1 + m_2$. For the material constants given in (7), the dimensionless effective mass m_{eff}/m_{st} is plotted in Fig. 5 as a function of ω/ω_0. Negative effective mass is seen to occur near the local resonance frequency ω_0. Besides, at the long

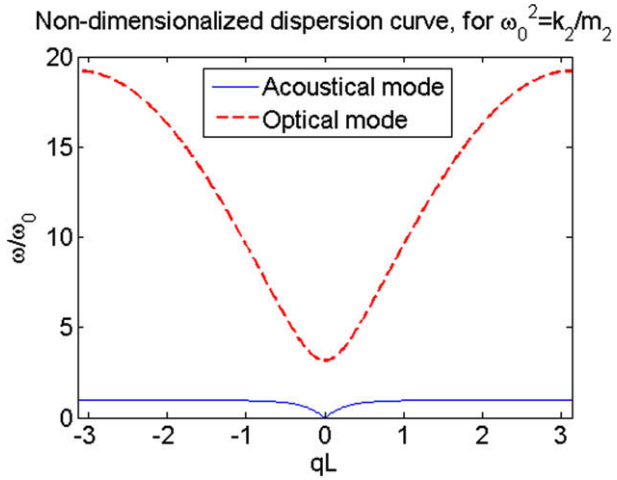

Fig. 3. Nondimensionalized dispersion curve for the mass-in-mass lattice model.

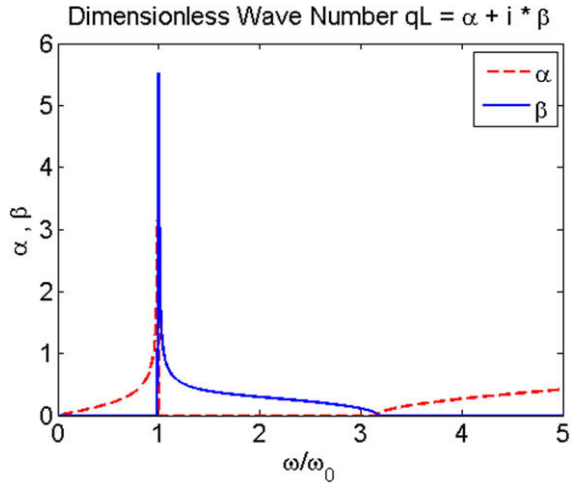

Fig. 4. Attenuation factor as a function of dimensionless frequency ω/ω_0.

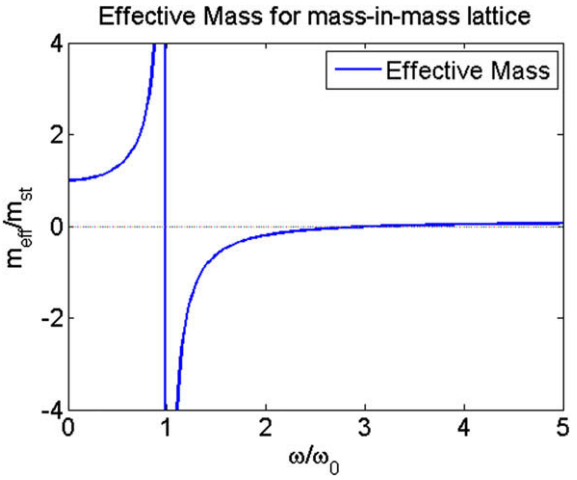

Fig. 5. Dimensionless effective mass m_{eff}/m_{st} as a function of ω/ω_0.

wavelength limit ($\omega \to 0$), the effective mass m_{eff} approaches m_{st} as expected. Since both k_1 and ω^2 are positive in (9), negative effective mass is possible only when $1 - \cos(qL)$ turns negative, i.e., the dimensionless wave number qL is complex. Hence, frequencies corresponding to negative mass lie in the stopping band. In other words, a negative effective mass in the equivalent mass-spring lattice system yields spatial attenuation in wave amplitude.

In summary, we have shown that, to use a monatomic lattice system to represent the mass-in-mass lattice system, the effective single mass in the equivalent system must be frequency dependent and allowed to become negative.

3. Continuum representation of the mass-in-mass system

For a more efficient description of general motions/deformations, materials composed of periodic microstructures are often modeled as homogeneous continuous media. In this section, we investigate the difference resulting from using the classical elastic solid and a microstructure continuum to represent, respectively, the 1D mass-in-mass lattice system.

3.1. Representation by a classical elastic solid

The mass-in-mass and the equivalent monatomic lattice models considered in Section 2 are discrete systems. The classical continuum theory cannot directly represent the original mass-in-mass system because of the additional degree of freedom of the internal mass m_2. However, the equivalent monatomic lattice system with effective mass m_{eff} can be represented by a one-dimensional elastic solid with a unit cross-sectional area. The effective Young's modulus E_{eff} is determined by considering the static stress-strain relation of a unit cell. We have

$$E_{eff} = Lk_1 \tag{11}$$

The equation of motion of the one-dimensional elastic solid is

$$E_{eff}\frac{\partial^2 u}{\partial x^2} = \rho_{eff}\frac{\partial^2 u}{\partial t^2} \tag{12}$$

in which ρ_{eff} is the effective mass density. For classical elastic solids, both the Young's modulus and mass density are constants and wave propagation in these solids is not dispersive. Assuming a harmonic wave solution $u = B^* e^{i(qx-\omega t)}$ for Eq. (12), we obtain

$$\omega^2 = \frac{k_1}{\rho_{eff}L}(qL)^2 \tag{13}$$

In order to make the continuum model equivalent to the mass-in-mass system, the effective mass density ρ_{eff} is chosen to be a function of frequency ω so that the relation between frequency and wave number (qL) obtained from Eq. (13) matches that from Eq. (6) for the original mass-in-mass system. Denoting $\theta = m_2/m_1$, $\delta = k_2/k_1$, $\omega_0^2 = k_2/m_2$, and the static mass density $\rho_{st} = (m_1 + m_2)/L$, we derive the dimensionless mass density ρ_{eff}/ρ_{st} as

$$\frac{\rho_{eff}}{\rho_{st}} = \frac{\theta}{\delta(1+\theta)(\omega/\omega_0)^2}\left\{\cos^{-1}\left\{1 - \frac{\delta}{2\theta}\frac{(\omega/\omega_0)^2[(\omega/\omega_0)^2 - (1+\theta)]}{(\omega/\omega_0)^2 - 1}\right\}\right\}^2 \tag{14}$$

The frequency dependent mass density therefore can be calculated for any given frequency. Again, it can be shown numerically that negative effective mass density occurs near the local resonance frequency. In fact, it is noted that the dimensionless effective mass density ρ_{eff}/ρ_{st} and the dimensionless effective mass presented in Fig. 5, although derived from two different models, are nearly identical.

3.2. Microstructure continuum model

The classical continuum theory is not adequate for describing the deformation of materials with microstructures if local deformation/motion in the microstructure is desired [16,17]. Microstructure continuum theories which employ additional kinematic variables are more suitable to represent the mass-in-mass system. In this study, we introduce a microstructure continuum model in the form of multiple displacement variables. For simplicity, we still consider the one-dimensional mass-in-mass lattice for illustrating the development of an approximate microstructure continuum that can be used to describe the motion/deformation of the lattice system.

Consider the unit cell in the mass-in-mass lattice as shown in Fig. 6. During a general motion, the deformation and kinetic energies in the unit cell are

$$W^{(j)} = \frac{1}{2}[k_1(u_1^{(j+1)} - u_1^{(j)})^2 + k_2(u_2^{(j)} - u_1^{(j)})^2] \tag{15}$$

and

$$T^{(j)} = \frac{1}{2}[m_1(\dot{u}_1^{(j)})^2 + m_2(\dot{u}_2^{(j)})^2], \tag{16}$$

respectively.

Let $u_1(x)$ and $u_2(x)$ be continuous functions which give the displacements of all m_1 and m_2 mass points, respectively. Using a two-term Taylor series expansion, we have

$$u_1^{(j+1)} = u_1(x+L) = u_1(x) + \frac{\partial u_1}{\partial x}L = u_1^{(j)} + \frac{\partial u_1}{\partial x}L \tag{17}$$

Note that the technique of expansion in (17) has been discussed in detail by Kunin [20]. Apparently, better approximation can be achieved if more terms are retained in the expansion. Using this technique Kunin transforms a discrete system into a quasi-continuum. However, in the present study we use the two-term Taylor series expansion to transform the lattice system into a nonclassical continuum which is able to closely account for most of the characteristics of the original discrete model.

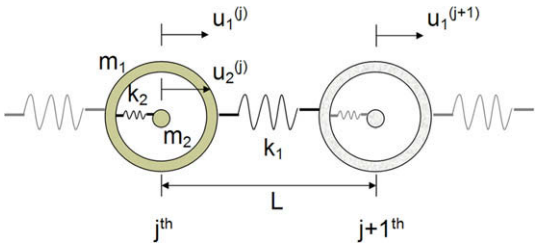

Fig. 6. Definition of variables for microstructure continuum model.

Let the one-dimensional equivalent continuum have a unit cross-sectional area. The deformation and kinetic energy densities for the equivalent continuum are obtained, respectively, from (15) and (16) as

$$W = \frac{1}{2L}\left[k_1\left(\frac{\partial u_1}{\partial x}L\right)^2 + k_2(u_2-u_1)^2\right] \tag{18}$$

$$T = \frac{1}{2L}[m_1(\dot{u}_1)^2 + m_2(\dot{u}_2)^2] \tag{19}$$

In deriving the equations above, the relation of (17) has been used.

The deformation energy density given by Eq. (18) can be used to establish the constitutive relations for the multi-displacement continuum model. We define normal strain $\varepsilon = \partial u_1/\partial x$ and relative strain $\varepsilon_R = (u_2 - u_1)/L$, then the deformation energy density W can be expressed solely in terms of the two strains. Subsequently, the Cauchy stress and relative stress are introduced by

$$\sigma = \frac{\partial W}{\partial \varepsilon} = k_1 L\varepsilon \tag{20}$$

and

$$\sigma_R = \frac{\partial W}{\partial \varepsilon_R} = k_2 L\varepsilon_R, \tag{21}$$

respectively. Eqs. (20) and (21) are the constitutive equations of the multi-displacement continuum model.

The final step to complete the continuum modeling is to derive the equations of motion using the Hamilton's principle

$$\delta\int_{t_0}^{t_1}\int_V (T-W)dVdt + \int_{t_0}^{t_1}\int_S T_i\delta u_i dAdt = 0 \tag{22}$$

We obtain

$$m_1\ddot{u}_1 - k_1L^2\frac{\partial^2 u_1}{\partial x^2} + k_2(u_1-u_2) = 0 \tag{23}$$

$$m_2\ddot{u}_2 + k_2(u_2-u_1) = 0 \tag{24}$$

The equations of motion above are partial differential equations at a point in the equivalent continuum and can be solved in the usual way. It is noted that in the multi-displacement continuum model, the degrees of freedom of the two masses are separately accounted for with the kinematic variable u_1 and u_2, respectively, and, thus, there is no need to use an effective mass in the model and the possibility of frequency dependent and negative effective mass is avoided.

3.3. Evaluation of the multi-displacement continuum model

It should be pointed out that, in deriving the multi-displacement continuum model, the only approximation made is the truncation of the Taylor expansion in Eq. (17). To evaluate the accuracy of the representation of the mass-in-mass system by the multi-displacement continuum model, we consider harmonic wave propagation of the form

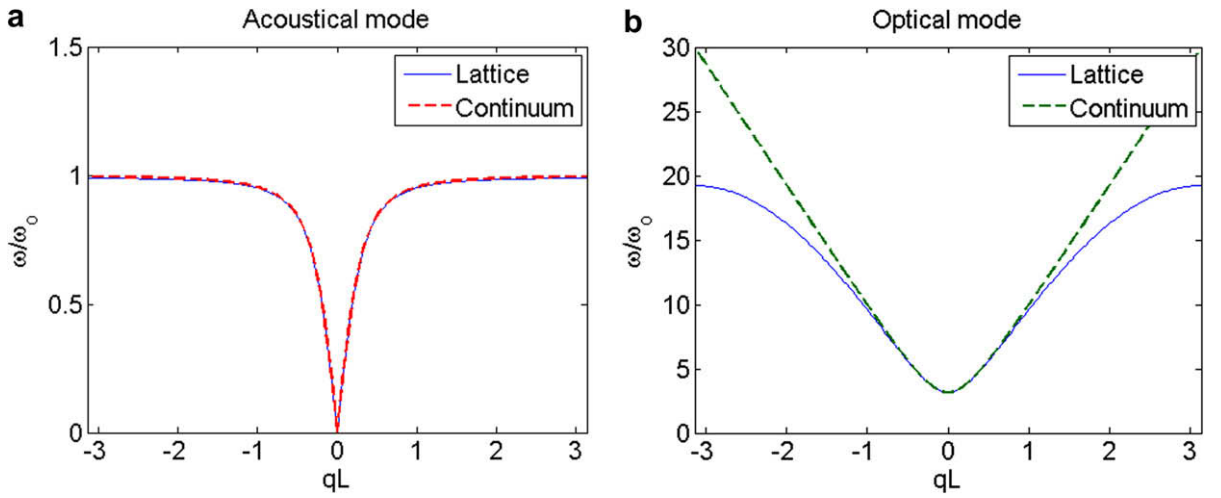

Fig. 7. Dispersion curve obtained from the multi-displacement continuum model compared with that from the mass-in-mass lattice model; (a) acoustical mode and (b) optical mode.

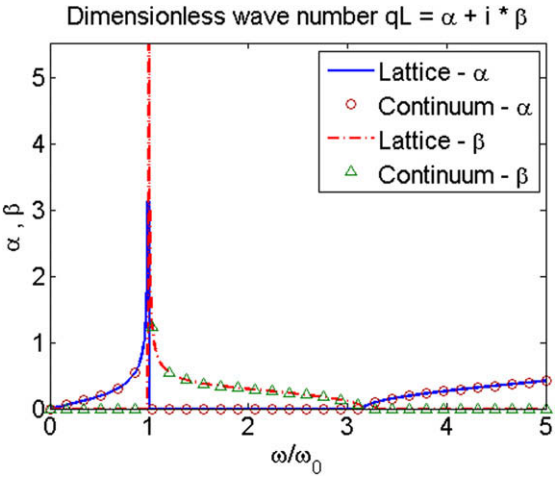

Fig. 8. Attenuation factor as a function of frequency for the multi-displacement continuum model compared with that for the lattice model.

$$u_\gamma = B_\gamma e^{i(qx-\omega t)} \quad ,\gamma = 1,2 \tag{25}$$

Substituting the expressions in the equations of motion Eq. (23) and (24), we obtain the dispersion equation as

$$m_1 m_2 \omega^4 - [(m_1+m_2)k_2 + m_2 k_1 (qL)^2]\omega^2 + k_1 k_2 (qL)^2 = 0 \tag{26}$$

In order to obtain a comprehensive comparison of the multi-displacement continuum model with the exact model over a wide range of frequencies, the dispersion curves are plotted in Fig. 7 using the material data of Eq. (7). It is evident that the multi-displacement continuum model describes the mass-in-mass system very well especially for the acoustical mode. As for the optical mode, the accuracy is fairly accurate up to $qL = \pi/2$. In view of the relation $q = 2\pi/wavelength$, we conclude that the multi-displacement continuum model is accurate for wavelengths greater than four times the lattice spacing (L) for the optical mode. Of interest to note is the close agreement between two solutions for attenuation factor β as shown in Fig. 8. This implies that the multi-displacement continuum model can also capture the characteristic mechanical phenomena of the original mass-in-mass lattice without the use of negative mass density over a wide frequency range including both passing and stopping bands.

4. Conclusion

From the study of wave propagation in a one-dimensional lattice system consisting of mass-in-mass units, it was found that near the local resonance frequency of the internal mass, spatial decay of wave amplitude occurs. If the lattice is modeled as a system of single mass units, the effective mass of the unit becomes negative for frequencies near the local resonance frequency. A similar phenomenon(negative mass density) exists if the lattice system is modeled as a classical elastic solid. Moreover, the effective mass density of the equivalent elastic solid is frequency dependent and has to be derived from the exact dispersion equation of the original lattice system. In contrast, the multi-displacement microstructure continuum model is able to capture the dynamic response of the mass-in-mass lattice system including the band gap structure without resorting to the use of the effective mass/mass density. In other words, no negative effective mass density occurs in the microstructure model. However, while the microstructure model predicts the acoustic mode accurately, the accuracy in predicting the optical mode is good only in a limited frequency range.

References

[1] V.G. Veselago, The electrodynamics of substances with simultaneously negative values of ε and μ, Sov. Phys. Usp. 10 (1968) 509–514.
[2] J.B. Pendry, Negative refraction makes a perfect lens, Phys. Rev. Lett. 85 (2000) 3966–3969.
[3] J. Valentine, S. Zhang, T. Zentgraf, E. Ulin-Avila, D.A. Genov, G. Bartal, X. Zhang, Three-dimensional optical metamaterial with a negative refractive index, Nature 455 (2008) 376–379.
[4] J. Li, C.T. Chan, Double-negative acoustic metamaterial, Phys. Rev. E 70 (2004) 055602.
[5] N. Fang, D. Xi, J. Xu, M. Ambati, W. Srituravanich, C. Sun, X. Zhang, Ultrasonic metamaterials with negative modulus, Nat. Mater. 5 (2006) 452–456.
[6] Y. Ding, Z. Liu, C. Qiu, J. Shi, Metamaterial with simultaneously negative bulk modulus and mass density, Phys. Rev. Lett. 99 (2007) 093904.
[7] Y. Cheng, J.Y. Xu, X.J. Liu, One-dimensional structured ultrasonic metamaterials with simultaneously negative dynamic density and modulus, Phys. Rev. B 77 (2008) 045134.
[8] C.T. Chan, Jensen Li, K.H. Fung, On extending the concept of double negativity to acoustic waves, JZUS A 7 (2006) 24–28.
[9] Z. Liu, X. Zhang, Y. Mao, Y.Y. Zhu, Z. Yang, C.T. Chan, P. Sheng, Locally resonant sonic materials, Science 289 (2000) 1734–1736.
[10] Z. Liu, C.T. Chan, P. Sheng, Analytic model of phononic crystals with local resonances, Phys. Rev. B 71 (2005) 014103.
[11] G.W. Milton, J.R. Willis, On modifications of Newton's second law and linear continuum elastodynamics, Proc. R. Soc. A 463 (2007) 855–880.
[12] B.S. Lazarov, J.S. Jensen, Low-frequency band gaps in chains with attached with non-linear oscillators, Int. J. Non-linear Mech. 42 (2007) 1186–1193.

[13] J.H. Vincent, On the construction of a mechanical model to illustrate Helmholtz's theory of dispersion, Philos. Mag. 46 (1898) 557–563.
[14] S. Yao, X. Zhou, G. Hu, Experimental study on negative mass effective mass in a 1D mass-spring system, New J. Phys. 10 (2008) 043020.
[15] E. Cosserat, F. Cosserat, Théorie des Corps Déformables, Hermann & Fils, Paris, 1909.
[16] C.T. Sun, G.L. Huang, Modeling heterogeneous media with microstructures of different scales, J. Appl. Mech. 74 (2007) 203–209.
[17] G.L. Huang, C.T. Sun, Continuum modeling of solids with micro/nanostructures, Philos. Mag. 87 (2007) 3689–3707.
[18] P. Sheng, X.X. Zhang, Z. Liu, C.T. Chan, Locally resonant sonic materials, Physica B 338 (2003) 201–205.
[19] L. Brillouin, Wave Propagation in Periodic Structures, Dover, New York, NY, 1953.
[20] I.A. Kunin, Elastic Media with Microstructure I & II, Springer-Verlag, Berlin, Heidelberg, New York, 1982–1983.